IJSEAT International Journal of Science Engineering and Advance Technology

Modeling and Simulation of Photovoltaic Fed Drive by Using High Voltage Gain DC-DC Boost Converter

Muralidhar A
M. Tech. Scholar,
Department of Electrical and Electronics Engineering,
Nova College of Engineering & Technology, JNTUK;
West Godavari (Dt); A.P, India.
muralidharannam@gmail.com

Peddakapu K
Assistant Professor
Department of Electrical and Electronics Engineering,
Nova College of Engineering & Technology, JNTUK;
West Godavari (Dt); A.P, India.
peddakapu45@gmail.com

***Abstract*— D.C. motors are seldom used in ordinary applications because all electric supply companies furnish alternating current. However, for special applications such as in steel mills, mines and electric trains, it is advantageous to convert low value of DC into high value of DC in order to use D.C. motors controlled by power electronic apparatus. Here the DC motor is controlled power electronic converters through RES system. The renewable energy sources such as PV modules, fuel cells or energy storage devices such as super capacitors or batteries deliver output voltage at the range of around 15 to 40 VDC. A boost converter is used to clamp the voltage stresses of all the switches in the interleaved converters, caused by the leakage inductances present in the practical coupled inductors, to a low voltage level. Overall performance of the renewable energy system is then affected by the efficiency of step-up DC/DC converters with closed loop control action, which are the key parts in the system power chain. This paper presents a dc-dc power converter integrated closed loop system to attain high stability factor in such a way to obtain, in a single stage conversion fed DC motor drive. This review is mainly focused on high efficiency step-up DC/DC converters with high voltage gain. The results are obtained through Matlab/Simulink software package.**

***Index Terms*— DC–DC Power Conversion, Capacitor Modules, Interleaved Methodology, PI Controller.**

I.INTRODUCTION

DC motors are used extensively in adjustable speed drives and position control applications. Their speeds below the base speeds can be controlled by armature/voltage control. Speeds above the base speed are obtained by field-flux control method. As speed control method for DC motors are simpler and less expensive than those for AC motors, DC motors are preferred where wide speed range control is required. For this control objective of DC drive is obtained by using power electronic device fed renewable energy generation scheme now implemented in many industrial applications. Fig. 1shows the schematic diagram that the PV panel is connected to the DC motor through proposed converter by a closed loop control. In recent years, there has been an upsurge of interest in solar photovoltaic (PV) energy systems in both industry and academia [1]-[4]. In typical PV power generation systems, several photovoltaic panels are connected in series and parallel to form an array and feed energy to a single centralized converter [16]. An alternative approach is to use a DC module, which is a combination of one PV panel and one power conditioning

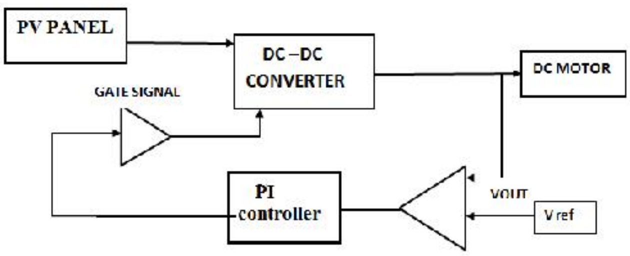

Fig.1 General Schematic of standalone system with closed loop control

unit, to feed power directly into the DC grid [8]. The advantages of a DC module based system over formal systems due to centralized control action are as follows:
1) The maximum power point (MPP) of each panel can be tracked individually, thereby increasing the utilization of the whole PV system;
2) Detrimental effects due to shading and module mismatches are not present.
3) Potential arcing problems due to DC system wiring are fully avoided.

A DC–DC converter with a high step-up voltage gain is used for many applications, such as high-intensity discharge lamp ballasts for automobile headlamps, fuel cell energy conversion systems, solar-cell energy conversion systems and battery backup systems for uninterruptible power supplies [9]-[12]. Theoretically, a dc–dc boost converter can achieve a high step-up voltage gain with an extremely high duty ratio. However, in practice, the step-up voltage gain is limited due to the effect of power switches, rectifier diodes and the equivalent series resistance (ESR) [13] of inductors and capacitors.

In general, a conventional boost converter can be adopted to provide a high step-up voltage gain with a large duty ratio. However, the conversion efficiency and the step-up voltage gain are limited due to the constraints of the losses of power switches and diodes, the equivalent series resistance of inductors and capacitors and the reverse recovery problem of diodes. However, the active switch of these converters will suffer very high voltage stress and high power dissipation due to the leakage inductance of the transformer. Although this configuration is useful in terms of system monitoring and repair, the partial shading, module mismatch, and dc connection cable losses are inevitable problems and lead to significantly reduced system energy yields [14]–[17].

The energy of a single PV panel through the converter output to the main electricity; this is a general DC grid-connected system. The converter is inlaid in the rear bezel of the PV panel and outputs the dc current to the load or to the main electricity; this alternative solution not only immunizes the yield loss by shadow effect, but also provides flexible installation options according to the user's budget [5]–[7]. The maximum power point (MPP) voltage range is from 15 V to 40 V with various power capacities of about 100 W to 300 W for a single commercial PV panel. When a wide input voltage range is essential for the single stage converter, high efficiency is difficult to achieve. However, the single stage conversion system, which combines a high step-up dc/dc converter, is able to achieve efficiency as high as the conventional PV string-type inverter [8]. The typical Zeta converter provides either a step-up or a step-down function to the output, in a manner similar to that of the buck-boost or SEPIC converter topologies [11]. The conventional Zeta converter is configured of two inductors, a series capacitor and a diode.

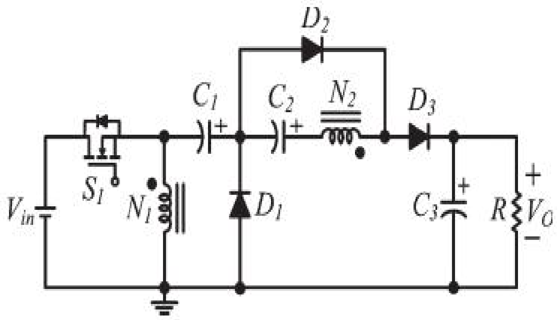

Fig. 2. Circuit Configuration of Proposed Converter.

However, leakage inductance issues that relate to the voltage spike and the efficiency remain significant. An integrated boost–fly back converter [13] based on a coupled inductor with high efficiency and high step-up voltage gain has been presented. The energy stored in the leakage inductor is recycled into the output during the switch off period [8]-[12]. Thus, the efficiency can be increased and the voltage stress on the active switch can be suppressed. Many step-up converters [14]-[15], which use an output voltage stacking to increase the voltage gain, are presented. This paper proposes the a new converter topology operated under closed loop control action by using PI controller to achieve high stability with low steady state error values and evaluated by using Matlab/Simulink platform.

II. PROPOSED CONVERTER TOPOLOGY

The simplified circuit model of the proposed converter is shown in Fig. 2. The coupled inductor T_1 includes a magnetizing inductor Lm, primary and secondary leakage inductors L_{k1} and L_{k2}, and an ideal transformer primary winding N_1 and secondary winding N_2. To simplify the circuit analysis of the proposed converter, the following assumptions are made.

1) All components are ideal, except for the leakage inductance of coupled inductor T_1.The ON-state resistance RDS (ON)and all parasitic capacitances of the main switch $S_1$are neglected, as are the forward voltage drops of the diodes D_1~D_3.

2) The capacitors C_1~C_3 are sufficiently large that the voltages across them are considered to be constant.

3) The ESR of capacitors C1~C3 and the parasitic resistance of coupled-inductor T1 are neglected.

4) The turns ratio n of the coupled inductorT1winding is equal to N_2/N_1.

The operating principles for continuous-conduction mode (CCM) are now presented in detail. Fig. 3 shows the typical waveform of several major components during one switching period. The five operating modes are described as follows.

CCM Operation

Mode I[t_0,t_1]: In this transition interval, the secondary leakage inductor L_{k2} is continuously releasing its energy to capacitor C_2. The current flow path is shown in Fig. 4(a); as shown, switch $S_1$and diodes $D_2$are conducting. The current i_{Lm} is descending because source voltage V_{in} is applied on

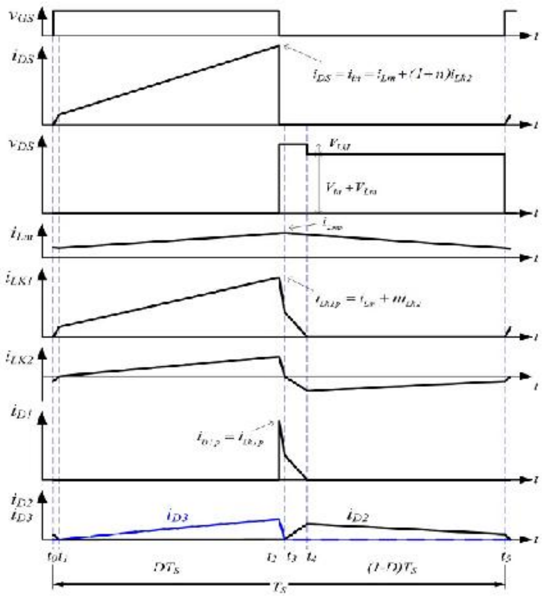

Fig.3 Typical waveforms of the proposed converter at CCM operation.

magnetizing inductor Lm and primary leakage inductorLk1; meanwhile, L_m is also releasing its energy to the secondary winding, as well as charging capacitor C2 along with the decrease in energy, the charging current iD2 and iC2 are also decreasing. The secondary leakage inductor current i_{LK2} is declining according to i_{Lm}/n. Once the increasing i_{Lk1}equals the decreasing i_{Lm} at $t=t_1$, this mode ends

$$i_{in}^{I}(t) = i_{DS}^{I}(t) = i_{LK1}^{I}(t) \tag{1}$$

$$\frac{di_{Lm}^{I}(t)}{dt} = \frac{v_{Lm}}{L_m} \tag{2}$$

$$\frac{di_{Lk1}^{I}(t)}{dt} = \frac{V_{in} - v_{Lm}}{L_{k1}} \tag{3}$$

$$i_{LK2}^{I}(t) = \frac{i_{Lm}(t) - i_{Lk1}(t)}{n} \tag{4}$$

Mode II[t1,t2]: During this interval, source energy Vin is series connected with C1,C2, secondary winding N2, and Lk2 to charge output capacitor C3 and load R; meanwhile, magnetizing inductor Lm is also receiving energy from Vin. The current flow path is shown in Fig.4(b); as illustrated, switchS_1 remains on, and only diodeD3is conducting. The i_{Lm}, i_{Lk1}, and i_{D3} are increasing because the V_{in} is crossing Lk1,Lm and primary winding N1;Lm and Lk1are storing energy from V_{in}; meanwhile, Vin is also in series with N_2 of coupled inductor T1, and capacitors $C_1$and$C_2$are discharging their energy to capacitor $C_3$and load R, which leads to increases in i_{Lm}, i_{Lk1}, i_{DS}, and i_{D3}.

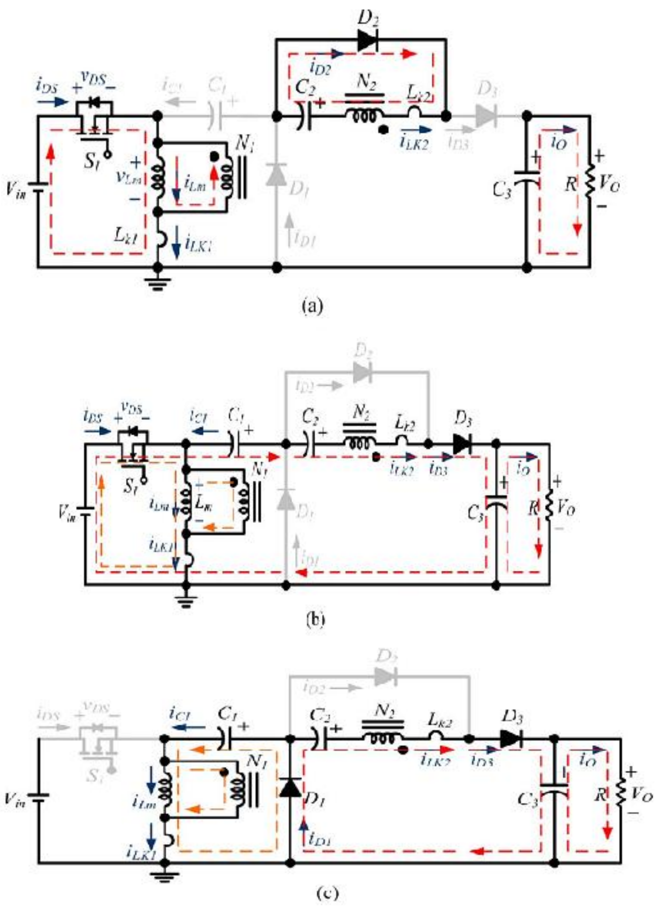

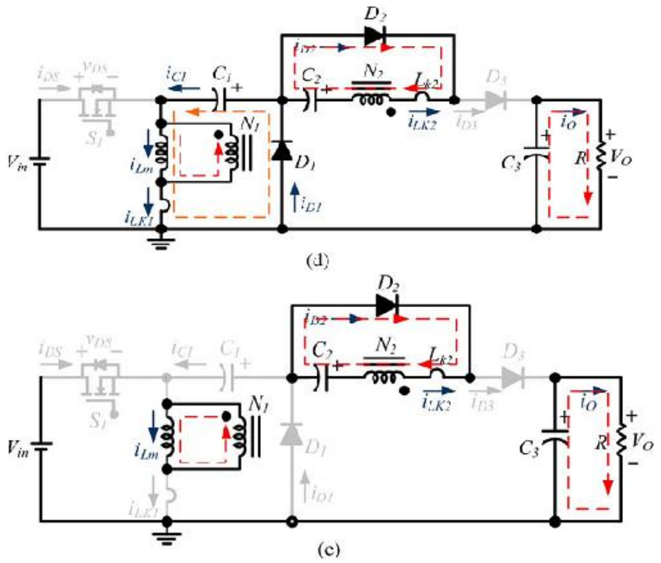

Fig.4. Current flow path in five operating modes during one switching period in CCM operation. (a) Mode I. (b) Mode II. (c) Mode III. (d) Mode IV. (e) Mode V.

This mode ends when switch $S_1$is turned off at t=t2

$$i_{Lm}^{II}(t) = i_{Lk1}^{II}(t) - n i_{LK2}^{II}(t) \tag{5}$$

$$\frac{di_{Lm}^{II}(t)}{dt} = \frac{v_{in}}{L_m} \tag{6}$$

$$i_{in}^{II}(t) = i_{DS}^{II}(t) = i_{Lm}^{II}(t) + (1+n) i_{LK2}^{II}(t) \tag{7}$$

$$\frac{di_{Lk2}^{II}(t)}{dt} = \frac{di_{D3}^{II}(t)}{dt} = \frac{(1+n)V_{in} + V_{C1} - V_{C2}}{L_{k2}} \tag{8}$$

Mode III[t_2,t_3]: During this transition interval, secondary leakage inductor Lk2 keeps charging C3 when switch S1 is off. The current flow path is shown in Fig. 4(c), and only diodes D1 and D3are conducting. The energy stored in leakage inductor L_{k1} flows through diode D1 to charge capacitor C1 instantly whenS1turns off. Meanwhile, the L_{k2} keeps the same current direction as in the prior mode and is in series with C2 to charge output capacitor C3 and load R. The voltage across S1is the summation of V_{in} , V_{Lm}, and V_{Lk1}. Currents i_{Lk1} and i_{Lk2} are rapidly declining, but i_{Lm} is increasing because Lm is receiving energy from L_{k2}. Once current i_{Lk2} drops to zero, this mode ends at t=t3

$$i_{in}^{III}(t) = 0 \tag{9}$$

$$i_{Lm}^{III}(t) = i_{Lk1}^{III}(t) - n i_{LK2}^{III}(t) \tag{10}$$

$$\frac{di_{Lk1}^{III}(t)}{dt} = \frac{-V_{C1} - V_{Lm}}{L_{k1}} \tag{11}$$

$$\frac{di_{Lk2}^{III}(t)}{dt} = \frac{di_{D2}^{III}(t)}{dt} = \frac{nV_{Lm}+V_{C2}-V_o}{L_{k2}} \quad (12)$$

Mode IV[t_3,t_4]: During this transition interval, the energy stored in magnetizing inductor Lm releases simultaneously to $C_1$and C_2. The current flow path is shown in Fig. 4(d). Only diodes D_1 and D_2 are conducting. Currents i_{Lk1} and i_{D1} are persistently decreased because leakage energy still flows through diode D1 and continues charging capacitorC1.The Lm is delivering its energy through T_1 and D_2 to charge capacitor C_2. The energy stored in capacitors C3is constantly discharged to the load R. The voltage across S1 is the same as previous mode. Currents iLk1 and i_{Lm} are decreasing, but i_{D2} is increasing. This mode ends when current i_{Lk1} is zero at t=t_4

$$i_{Lm}^{IV}(t) = i_{Lk1}^{IV}(t) - ni_{LK2}^{IV}(t) \quad (13)$$

$$\frac{di_{Lk1}^{IV}(t)}{dt} = \frac{-V_{C1}-V_{Lm}}{L_{k1}} \quad (14)$$

$$\frac{di_{Lk2}^{IV}(t)}{dt} = \frac{V_{C2}+nV_{Lm}}{L_{k2}} \quad (15)$$

Mode V[t_4,t_5]: During this interval, magnetizing inductor L_m is constantly transferring energy to C2. The current flow path is shown in Fig. 4(e), and only diode D_2 is conducting. The i_{Lm} is decreasing due to the magnetizing inductor energy flowing continuously through the coupled inductor T_1 to secondary winding N_2 and D_2 to charge capacitor C_2. The energy stored in capacitors$C_3$is constantly discharged to the load R. The voltage acrossS1is the summation of V_{in} and V_{Lm}. This mode ends when switchS1is turned on at the beginning of the next switching period

$$\frac{di_{Lm}^{V}(t)}{dt} = \frac{V_{Lm}}{L_m} \quad (16)$$

$$i_{Lk1}^{V}(t) = 0 \quad (17)$$

$$\frac{di_{Lk2}^{V}(t)}{dt} = \frac{nV_{Lm}+V_{C2}}{L_{k2}} \quad (18)$$

III. STEADY-STATE ANALYSIS

CCM Operation

To simplify the steady-state analysis, only modes II and IV are considered for CCM operation, and the leakage inductances at primary and secondary sides are ignored. The following equations can be written from Fig. 4(b):

$$v_{Lm} = v_{in} \quad (19)$$

$$v_{N2} = nv_{in} \quad (20)$$

During mode IV, the following equations can be written:

$$v_{Lm} = -V_{c1} \quad (21)$$

$$-v_{N2} = V_{c2} \quad (22)$$

Applying a volt-second balance on the magnetizing inductor Lm yields

$$\int_0^{DT_s} V_{in}\,dt + \int_{DT_s}^{T_s} -V_{C1}\,dt = 0 \quad (23)$$

$$\int_0^{DT_s} nV_{in}\,dt + \int_{DT_s}^{T_s} -V_{C2}\,dt = 0 \quad (24)$$

from which the voltage across capacitor C1and C2 are obtained as follows:

$$V_{c1} = \frac{D}{1-D}V_{in} \quad (25)$$

$$V_{c1} = \frac{nD}{1-D}V_{in} \quad (26)$$

During mode II, the output voltage V_O=V_{in}+V_{C1}+V_{N2}+ V_{C2},as shown

$$V_o = v_{in} + nv_{in} + \frac{D}{1-D}V_{in} + \frac{nD}{1-D}V_{in} \quad (27)$$

The dc voltage gain MCCM can be found as follows:

$$M_{CCM} = \frac{V_o}{V_{in}} = \frac{I_{in}}{I_o} = \frac{1+n}{1-D} \quad (28)$$

voltage gain MCCM as a function of duty ratio D by various turns ratios, and the straightness of the curve accounts for the correction between turns ratio n and duty ratio under the voltage gain MCCM=8. The plot of voltage gain MCCM as a function of duty ratio D of the proposed converter is compared with three different converters [26], [27]-[33]; all are under CCM operation and n=3.

IV. PI CONTROLLER SYSTEM:

A proportional-integral controller (PI controller) is a generic control loop feedback mechanism (controller) widely used in industrial control systems.

The error signal is obtained by sampling the output voltage of the proposed converter and comparing it with a constant reference value. This error signal is processed by using PI controller and its output is used as reference signal to generate the gating pulses for switching devices.

The equation for the PI controller with its transfer function is studied. The signal (u) just past the controller is now equal to the proportional gain (K_p) times the magnitude of The error plus the integral gain (K_i) times the integral of the error.

$$\frac{K_I}{S} + K_p = \frac{K_I + SK_p}{S} \tag{29}$$

The values of K_p and K_I are taken as 0.2 and 0.5.

V. MATLAB MODELLING AND SIMULATION RESULTS

Here the simulation is carried out by two cases, in that

1. Proposed DC/DC Converter Operating Under Open Loop Condition.
2. Proposed DC/DC Converter Operating Under Closed Loop Condition with DC Drive.

Case 1: Proposed DC/DC Converter Operating Under Open Loop Condition

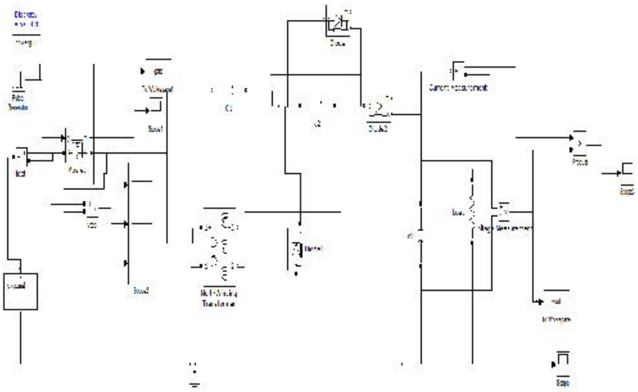

Fig.5 Matlab/Simulink Model of Proposed DC/DC Converter Operating Under Open Loop Condition

Fig.5 shows the Matlab/Simulink Model of Proposed DC/DC Converter Operating under Open Loop Condition using Matlab/Simulink Tool.

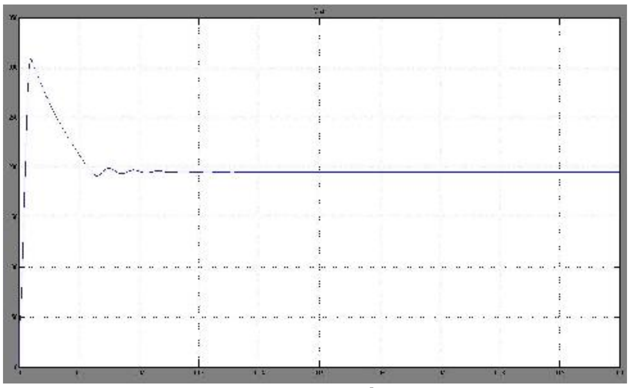

Fig.6 Output Voltage

Fig.6 shows the Output Voltage of Proposed DC/DC Converter Operating under Open Loop Condition, due to non-presence of feedback system attains low stable operation, attains 0.02 sec for fast response.

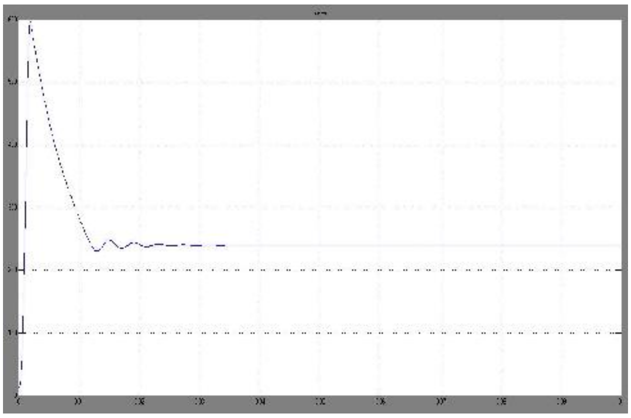

Fig.7 Output Power

Fig.7 shows the Output Power of Proposed DC/DC Converter Operating under Open Loop Condition.

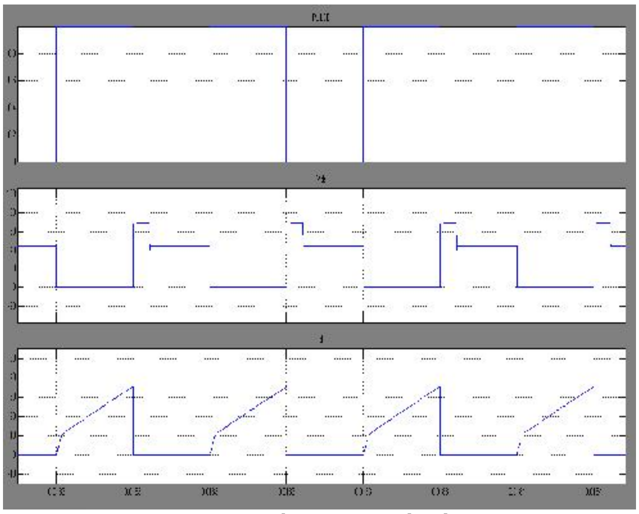

Fig.8 Switching States, Vds, Ids

Fig.8 shows the Switching States, Vds, Ids of Proposed DC/DC Converter Operating under Open Loop Condition.

Case 2: Proposed DC/DC Converter Operating Under Closed Loop Condition with DC Drive

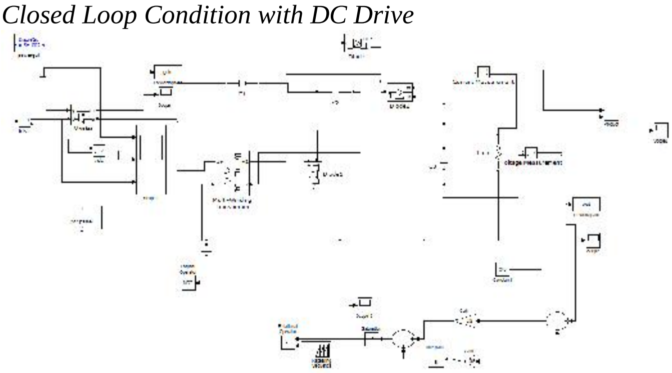

Fig.9 Matlab/Simulink Model of Proposed DC/DC Converter Operating Under Closed Loop Condition

Fig.9 shows the Matlab/Simulink Model of Proposed DC/DC Converter Operating under Closed Loop Condition using Matlab/Simulink Tool.

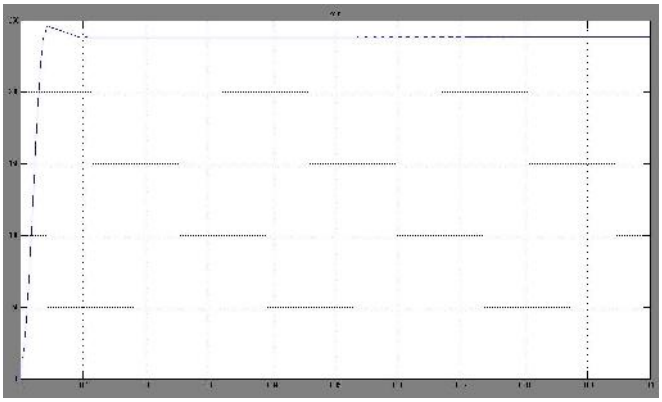

Fig.10 Output Voltage

Fig.10 shows the Output Voltage of Proposed DC/DC Converter Operating under Closed Loop Condition, due to presence of feedback system attains high stable operation, attains 0.01 sec for fast response.

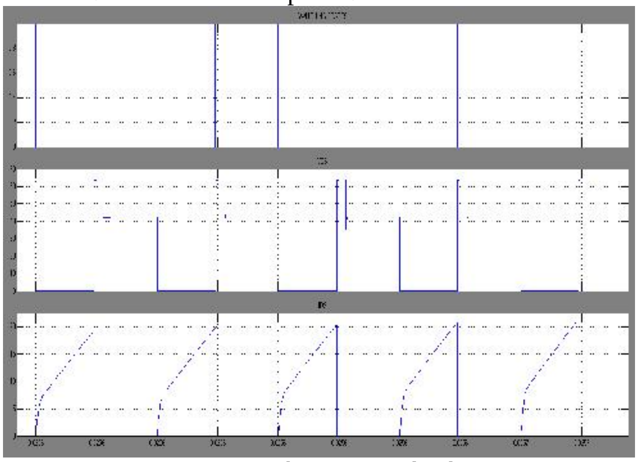

Fig.10 Switching States, Vds, Ids

Fig.10 shows the Switching States, Vds, Ids of Proposed DC/DC Converter Operating under Closed Loop Condition.

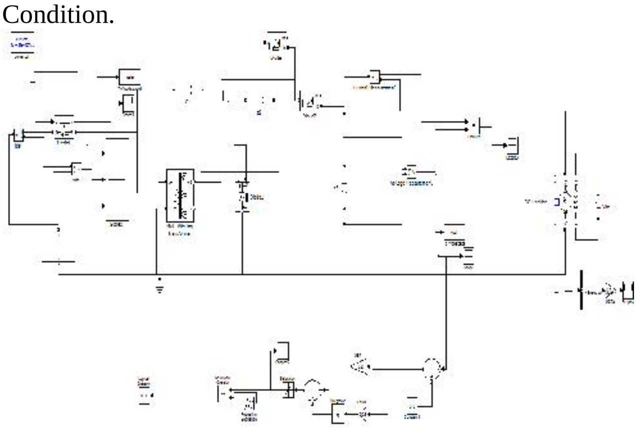

Fig.11 Matlab/Simulink Model of Proposed DC/DC Converter Operating Under Closed Loop Condition Fed DC Drive

Fig.11 shows the Matlab/Simulink Model of Proposed DC/DC Converter Operating under Closed Loop Condition fed DC drive using Matlab/Simulink Tool.

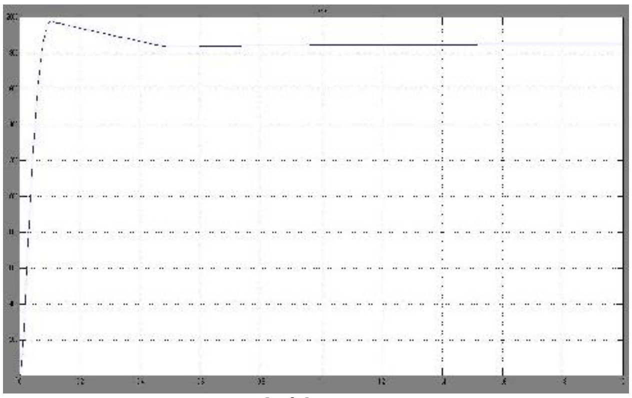

Fig.12 Speed of the DC Drive System

Fig.12 Speed of Proposed DC/DC Converter Operating under Closed Loop Condition fed DC drive.

V. CONCLUSION

Since DC power sources are widely used in many applications, including DC power supplies, battery chargers, and lighting systems .The high step up dc–dc converters are usually used as the front-end converters to step-up from low voltage to high voltage which are required to have a large conversion ratio, high efficiency, and small volume The proposed converter employs the turns ratio n=3 of the coupled inductor to achieve 8 times step-up voltage gain; The energy of the leakage inductor of the coupled inductor is recycled, and the voltage stress across the active switch S_1 has been limited; these merits mean low ON-state resistance RDS (ON)can be selected, which effectively improves the efficiency of the proposed converter and uncertainties in the input can be compensated to controlling the steady state error by using closed loop PI controller system and induce to many industrial applications.

REFERENCES

[1] Global Market Outlook for Photovoltaics Until 2014, Eur. Photovoltaic Ind. Assoc. (EPIA), Brussels, Belgium, May 2010. [Online]. Available: http://www.epia.org/fileadmin/EPIA_docs/public/Global_Market_Outlook_for_Photovoltaics_until_2014.pdf

[2] Grid-connected versus stand-alone energy systems for decentralized power—A review of literature by Deepak Paramashivan Kaundinya*, P. Balachandra, N.H. Ravindranath

[3] A Review of Single-Phase Grid-Connected Inverters for Photovoltaic Modules by Soeren Baekhoej Kjaer, Member, IEEE, John K. Pedersen, Senior Member, IEEE, and Frede Blaabjerg, Fellow, IEEE

[4] Flyback-Type Single-Phase Utility Interactive Inverter With Power Pulsation Decoupling on theDC Input for an AC Photovoltaic Module System by Toshihisa Shimizu, Senior Member, IEEE, Keiji Wada, Member, IEEE, and Naoki Nakamura

[5] B. Axelrod, Y. Berkovich, and A. Ioinovici, ―Transformerless dc-dc converters with a very high dc line-to-load voltage ratio,‖ in Proc. IEEEISCAS, 2003, vol. 3, pp. 435–438.

[6] Design of low cost universal artificial neuron controller for chopper fed embedded DC drives by N. Senthil Kumara, V. Sadasivam, H.M. Asan Sukriya, S. Balakrishnan

[7] R.Sudha,Ms.Ashly Mary Tom and M.Sasikumar (2012), ‗An Efficient Non Isolated ZVT Boost Converter With A Single Resonant Inductor for Drive Applications,' International Journal of Knowledge Engineering and Research, Vol.1, Issue 2 , Pp. 76-80.

[8] A Boost Converter With Capacitor Multiplier and Coupled Inductor for AC Module Applications Shih-Ming Chen,Student Member, IEEE, Tsorng-Juu Liang,Senior Member, IEEE,Lung-Sheng Yang, and Jiann-Fuh Chen,Member, IEEE IEEE transactions on industrial electronics, vol. 60, no. 4, april2013

[9] B. R. Lin and F. Y. Hsieh, ―Soft-switching Zeta-flyback converter with abuck-boost type of active clamp,‖ IEEE Trans. Ind. Electron., vol. 54,no. 5, pp. 2813–2822, Oct. 2007.

[10] H.-L. Do, ―Zero-voltage-switching synchronous buck converter with a coupled inductor,‖ IEEE Trans. Ind. Electron., vol. 58, no. 8, pp. 3440–3447, Aug. 2011

[11] B. Axelrod, Y. Berkovich, S. Tapuchi, and A. Ioinovici, ―Steep conversionration C´ uk, Zeta, and sepic converters based on a switchedcoupled-inductor cell,‖ in Proc. IEEE Power Electron. Spec. Conf., 2008,pp. 3009–3014.

[12] H.-L. Do, ―Zero-voltage-switching synchronous buck converter with a coupled inductor,‖ IEEE Trans. Ind. Electron., vol. 58, no. 8, pp. 3440–3447, Aug. 2011

[13] Design Optimization for AsymmetricaI ZVS- PWM converter by TSAI-FU WU, Senior Member, IEEE SHIH-AN LJANG, Student Member, IEEE YAOW-MING CHEN, Member, IEEE

[14] D. Murthy-Bellur and M. K. Kazimierczuk, ―Two-transistor Zeta-flyback dc-dc converter with reduced transistor voltage stress,‖ Electron. Lett.,vol. 46, no. 10, pp. 719–720, May 2010

[15] J. Falin, ―Designing dc/dc converters based on ZETA topology, ‖AnalogAppl.J.,pp.16–21,2Q,2010.[Online]. Available:http://focus.ti.com/lit/an/slyt372/slyt372.pdf

[16] Voltage control of stand-alone wind and solar energy system by S.G. Malla, C.N. Bhende

MURALIDHAR A currently pursuing his M.Tech in Power Electronics & Drives from Nova College of Engineering & Technology, West Godavari (Dt), A.P, India, affiliated to JNTU, Kakinada. He has done his B.Tech degree from Regency Institute of Technology, Yanam, affiliated to Pondicherry University and his fields of interest include Photovoltaic Systems, Drives and Converters.

PEDDAKAPU K presently works as Assistant Professor in Nova College of Engineering & Technology, West Godavari (Dt), A.P, India. He has done his ME degree in Power Electronics from SRKR Engineering College Bhimavaram. His area of interest in Power Electronics, Renewable Energy Sources and Converters.